Title:

Protein nitration profile of T-cells from Alzheimer disease patients: Novel hints on immunosenescence and biomarker detection.

Authors:

Antonella Tramutola[1]*, Giulia Abate[2]*, Chiara Lanzillotta[1], Francesca Triani[1], Eugenio Barone[1], Federica Iavarone[3], Federica Vincenzoni[3], Massimo Castagnola[3], Mariagrazia Marziano[2], Maurizio Memo[2], Emirena Garrafa[2], D. Allan Butterfield[4], Marzia Perluigi[1], Fabio Di Domenico[1§], Daniela Uberti[2§]

Affiliations:

[1] Department of Biochemical Sciences, Sapienza University of Rome, Rome, Italy

[2] Department of Biomedical Sciences and Biotechnologies, University of Brescia, Brescia, Italy

[3] Istituto di Biochimica e Biochimica Clinica, Università Cattolica, and/or Dip. di Diagnostica di Laboratorio e Malattie Infettive, Fondazione Policlinico Universitario A.Gemelli, IRCCS, Rome-Italy

[4] Department of Chemistry and Sanders-Brown Center on Aging, University of Kentucky, Lexington, KY, USA

*Authors contributed equally to this work

§ Co-corresponding authors

Corresponding Authors:

Daniela Uberti, PhD

Department of Molecular and Translational Medicine,

University of Brescia, 25123 Brescia, Italy;

daniela.uberti@unibs.it

Fabio Di Domenico, PhD

Department of Biochemical Sciences,

Sapienza University of Rome, P.le Aldo Moro 5, Rome, Italy, 00185
fabio.didomenico@uniroma1.it

ABSTRACT

Alzheimer's disease (AD) is a progressive form of dementia characterized by increased production of amyloid-β plaques and hyperphosphorylated tau protein, mitochondrial dysfunction, elevated oxidative stress (OS), reduced protein clearance, among other. Several studies showed systemic modifications of immune and inflammatory systems due, in part, to decreased levels of T-cells in peripheral blood in AD. Considering that oxidative stress, both in the brain and in the periphery, can influence the activation and differentiation of T-cells, we investigated the 3-nitrotyrosine (3-NT) proteome of blood T-cells derived from AD patients compared to non-demented (ND) subjects by using a redox proteomic approach. 3-NT is a formal protein oxidation and index of nitrosative stress. We identified ten proteins showing increasing levels of 3-NT in T-cells from AD patients compared with ND subjects. These proteins are involved in energy metabolism, cytoskeletal structure, intracellular signaling, protein folding and turnover, and antioxidant response and provide new insights into the molecular mechanism that impact reduced T-cell differentiation in AD. Our results highlight the role of peripheral OS in T-cells related to immune-senescence during AD pathology focusing on the specific targets of protein nitration that conceivably can be suitable to further therapies. Further, our data demonstrate common targets of protein nitration between the brain and the periphery, supporting their significance as disease biomarkers.

Keywords: Alzheimer's disease; protein nitration; T-cells; oxidative stress; immunesenescence; proteomics.

INTRODUCTION

Alzheimer's disease (AD) is a neurodegenerative disorder, with a complex interplay of genetic and biochemical factors that contribute to the global cognitive deterioration associated with this disorder. The two main neuropathological hallmarks characterizing AD are extracellular senile plaques, resulting to extracellular misfolding and aggregation of amyloid beta peptides (Aβ), and neurofibrillary tangles composed of aggregated hyper-phosphorylated tau protein intracellularly [1]. Over the past twenty years "the A□ cascade hypothesis", derived from the discovery, of rare mutations harbored in three causative genes linked with increased Aβ□load (APP, PS1 and PS2), has dominated AD research and still plays a major role in pharmaceutical product pipelines [2, 3]. However, Aβ-centric approaches gave rise a degree of skepticism, suggesting that other main players of the disease can intertwine with amyloidogenic processes [4]. The fact that the disease takes many years before causing a manifest cognitive damage and aging is considered the most important risk factor for AD, suggests a multifactorial complexity, involving several independent events with interconnecting pathways [5].

It is noteworthy that several mechanisms involved in aging process, such as chronic inflammation and oxidative damage, are also common features of AD [6-8]. Numerous experimental and clinical evidences reported that inflammatory processes and dysregulation of redox homeostasis, with an increase of free radicals and a decrease of antioxidant defense capacity, are involved in the early stage of AD, even before the appearance of clinical symptoms [9, 10]. In addition, it is now well recognized that these two events are not only limited to the brain but have a systemic implication for the disease. Systemic modifications of immune and inflammatory systems have been reported in patients affected by AD, including: i) the decrease of B cells repertoire, with a reduced quality of antibody response [6, 10, 11]; ii) the remodeling of the T-cells pool with an accumulation of differentiated memory cells [12] and iii) the profound modification of the cytokine network, with increased circulating pro-inflammatory cytokines [11, 13-15]. Similarly, reduced antioxidant defenses have been found in peripheral cells of AD [16, 17] . Recently, investigating the redox steady state alterations in AD blood, we demonstrated decreased Superoxide Dismutase (SOD) enzyme activity and increased unfolded p53

isoform derived from redox-posttranslational modifications that made the protein to lose its native conformation and biological function [18-20]. In fact, p53 is a redox high sensitive protein involved in a myriad of cellular functions, including the regulation of innate immunity, by acting as a negative regulator of inflammation [21, 22].

In addition, by redox proteomics, we analyzed protein carbonylation of plasma proteins in mild cognitive impairment (MCI) and AD subjects demonstrating the alterations of proteins acting as extracellular chaperones, which may lead to the accumulation of oxidized products at the periphery [23].

The concept of chronic or prolonged free radical production (ROS/RNS) is considered central to the progression of chronic inflammation [24]. ROS/RNS can act both as mediators of inflammation, sustaining released of pro-inflammatory cytokines, and as second messengers for complete T-cells activation and differentiation [24, 25]. An additional signal for the induction of T-cell subset response is given by nitric oxide (NO), that combined with superoxide can produce peroxynitrite (ONOO-) and other RNS contributing to exacerbate nitro-oxidative stress [26].

Considering the increase amount of activated memory T-cells (CD45RO+) found in AD patients [12, 27, 28] and the high levels of NO described in the disease [8, 29-31], these subcellular population could be suitable for investigating the nitrated proteome and giving further insights into the mechanisms contributing to immunosenscence in AD pathology. Therefore, this current study investigated the nitro-oxidized proteome of blood T-cells derived from AD patients comparing them with those of non-demented (ND) subjects by using a redox proteomics approach.

MATERIALS AND METHODS

Subjects

Patients affected by Alzheimer's disease (n=19) and healthy age-matched ND subjects (n=19) were enrolled at the nursing home "Le Rondini" (Lumezzane, Italy). ND subjects recruited had to meet the following criteria: 1) no history of past or current psychiatric or neurologic disorders, and 2) a score higher than 26 in the Mini-Mental State

Examination (MMSE). The patients received a diagnosis of probable or possible AD according to NINCDS/ADRDA criteria (National Institute of Neurological and Communicative Disorders and Stroke/Alzheimer's Disease and Related Disorders Association). The Ethical Committee ASL-Brescia approved the protocol of this study (prot. n.0010771 dated 23/01/2013) and a written consent was obtained from all subjects or, where appropriate, their caregivers. Blood samples were collected in the morning and centrifuged immediately. Peripheral blood mononuclear cells (PBMCs) were obtained by Ficoll-Hypaque density gradient centrifugation (GE Healthcare, Little Chalfont, United Kingdom), and subsequently processed for mononuclear cells fractionation. Commercially available assay for clinic diagnostic use was employed to evaluate high sensitive CRP (hsCRP) plasma levels (immunoassay techniques; Siemens) by the Laboratory of Clinical Chemistry at Spedali Civili of Brescia. Table 1 reports the demographic/clinical characteristics of the donors and the levels of hsCRP.

Lymphocytes T-cells magnetic cell fractionation

$CD3^+$ T-cells were isolated using anti-$CD3^+$ magnetic microbeads (Miltenyi Biotec) and MACS columns (purity was >95%). Peripheral Blood Mononuclear Cells were resuspended in MACS buffer containing PBS pH 7.2, 0.5% BSA and 2 mM EDTA. $CD3^+$ MicroBeads were added to the cells and incubated for 20 minutes at 4°C. After the incubation period, the magnetic complex was passed over a separation column (MS Midi MACS), and placed in the magnetic field of a MACS Separator. Magnetically labeled $CD3^+$ T-Cells were retained in the MS Columns, while other cells were efficiently washed away with 5 washes using MACS buffer. Subsequently the column was removed from the magnetic field and placed on a suitable collection tube. The selected magnetically labeled-$CD3^+$ cell fraction was eluted by adding an appropriate amount of MACS buffer, by firmly applying the plunger. $CD3^+$ T-cells were lysed in immunoprecipitation buffer (10 mM Tris, pH 7.6; 140 mM NaCl; and 0.5% NP40 including protease inhibitors) for 20 min on ice, and cell debris was cleared by centrifugation.

Isolation of 3-NT modified proteins from $CD3^+$ T-cells

To analyze $CD3^+$ T-cells 3-NT-nitrated proteome, we immunoprecipitated 3-NT-proteins with μMACS Protein A/G MicroBeads (MACS Technology, Miltenyi Biotec). Specifically, 50 μg of protein extracts were incubated once for 30 minutes with 100 μL of the μMACS Protein A/G MicroBeads coated with 1 μg of anti-3-NT antibody (Sigma-Aldrich, St. Louis, MO, USA). After the incubation period, the magnetic immune-complex was passed over a separation column and placed in the magnetic field of a MACS Separator. At this stage magnetically labeled proteins were retained in the μcolumns, while other proteins were efficiently washed away with 5 washes using a Wash Buffer [0.15 M NaCl; 1% NP-40; 0.1%SDS; 0.5% Sodium Deoxycholate; 50mM Tris-HCl pH 8]. At the end of the washes the samples were eluted in IsoElectricFocusing (IEF) buffer. The final solution contained the 3-NT-enriched fraction. To obtain a total of 6 samples with a sufficient amount of protein (150 μg) to be used for IEF, we pooled the samples according with the clinical diagnosis (pathology score), age and sex (5 pools of 3 samples each and 1 pool of 4 samples).

Two-dimensional (2D) electrophoresis

For the first-dimension electrophoresis, approximately 200 μl of sample from AD and ND subjects were applied to 110-mm pH 3–10 IPG® ReadyStrip (Bio-Rad, Hercules CA). The strips were then actively rehydrated in the protean isoelectric focusing (IEF) cell (Bio-Rad) at 50 V for 18 h. The isoelectric focusing was performed in increasing voltages as follows; 300 V for 1 h, then linear gradient to 8000 V for 5 h and finally 20 000 V/h. Strips were then stored at −80 °C until the 2D electrophoresis was performed. For the second dimension, the IPG® Strips, were thawed and equilibrated for 10 min in 50 mM Tris–HCl (pH 6.8) containing 6 M urea, 1% (w/v) sodium dodecyl sulfate (SDS), 30% (v/v) glycerol, and 0.5% dithiothreitol, and then re-equilibrated for 15 min in the same buffer containing 4.5% iodacetamide instead of dithiothreitol. Linear gradient precast criterion Bis-Tris gels (12%) (Bio-Rad) were used to perform second dimension electrophoresis. Precision Protein™ Standards (Bio-Rad, CA) were run along with the samples at 200 V for 50 min. For the detection of 3-NT modified proteins, the gels were incubated in fixing solution (10% acetic acid, 40% methanol) for 40 min and stained

overnight at room temperature with 50 mL SYPRO Ruby gel stain (Bio-Rad). The SYPRO Ruby gel stain was then removed and the gels stored in deionized water.

Image analysis

SYPRO ruby-stained gel images were obtained using a Chemidoc MP System (Bio-Rad). All the images were saved in TIFF format. Gel imaging was software-aided using PD-Quest (Bio-Rad) imaging software. Briefly, a master gel was selected followed by normalization of all gels (ND and AD) according to the total spot density. Gel-to-gel analysis was then initiated in two parts. First, manual matching of common spots that could be visualized among the differential 2D gels was performed. After obtaining a significant number of spots the automated matching of all spots was then initiated. Automated matching is based on user-defined parameters for spot detection. These parameters are based on the faintest spot, the largest spot, and the largest spot cluster that occur in the master gel and are defined by the user. Based on these parameters the software defines spot centers for the gel. This process generates a large pool of data, approximately 400 spots. Only proteins showing computer-determined significant differential levels between the groups being analyzed were considered for identification. To determine significant differential levels of proteins, analysis sets were created using the analysis set manger software incorporated into the PD-Quest software. The numbers of pixels that occur in a protein spot were computed by the software corresponding to an increase/decrease in protein level. The gel image analysis was conducted first on Sypro Ruby-stained 3-NT gels and then on Sypro Ruby-stained expression gels. The two analyses were compared by software to normalize 3-NT value to expression value for each spot matched. A quantitative analysis set was created that recognized matched spots with differences in 3-NT intensity (normalized to expression intensity) that occur in each spot and a statistical analysis set was created that used a Student's t-test at 95% confidence to identify spots with p-values of $p < 0.05$. Spots with $p < 0.05$ were considered significant. A Boolean analysis set was created that identified overlapping spots from the aforementioned quantitative and statistical sets. These spots were selected for subsequent mass spectrometric analysis.

In-gel trypsin digestion/peptide extraction

Protein spots identifies as significantly altered from the comparison of two groups (AD and ND subjects) were excised from 2D-gels and transferred to individual Eppendorf microcentrifuge tubes for trypsin digestion as described previously [32]. In brief, DTT and IA were used to break, and cap disulfide bonds and the gel plug was incubated overnight at 37°C with shaking in modified trypsin solution. Tryptic peptide solutions were reconstituted in water and stored at −80° C until MS/MS analysis.

RP-HPLC-high resolution MS/MS characterization of tryptic peptides

High-resolution HPLC-ESI-MS/MS experiments were carried out by an Ultimate 3000 RSLCnano system coupled to an LTQ Orbitrap ELITE apparatus (Thermo Fisher Scientific, Waltham, MA, USA). PepMap RSLC C18 (2 μm particle diameter; 100 Å, column dimension 50 μm × 150 mm) (Thermo Scientific, Waltham, MA, USA) was used as chromatographic column. The following eluents were used: (A) 0.1% (v/v) aqueous FA and (B) 0.1% (v/v) FA in ACN. The applied gradient was: 0-7 min 3% B, 7-35 min from 3 to 55% B (linear), 35-36 min from 55 to 90% B (linear), at a flow rate of 0.3 μL/min with a total run of 60 min. MS spectra were collected with 60,000 resolution and m/z range from 300 to 2000. In data-dependent acquisition mode the five most intense multiply-charged ions were selected and fragmented in ion trap by using CID 35% normalized collision energy. Tuning parameters were: capillary temperature 250 °C, source voltage 2.10 kV.

MS data analysis

MS/MS data were elaborated by Proteome Discoverer software (version 1.4.1.14, Thermo Fisher Scientific, Waltham, MA, USA), based on SEQUEST HT cluster as search engine against UniProtKB mouse database (released on 15 of February 2017, Homo Sapiens 20168 entries). The search parameters were 10 ppm tolerance for precursor ions and 0.5 Da for product ions, 2 missed cleavage, Nitrosylation (+28,990 Da) of cysteine as variable modification. Protein characterization was set with the identification of a minimum of two unique peptides per protein applying the high confidence filter.

Slot blot

For the analysis of total 3-NT 10 µl of sample homogenate was incubated with 10 µl of Laemmli buffer containing 0.125 M Tris base pH 6.8, 4% (v/v) SDS, and 20% (v/v) glycerol. The resulting samples (250 ng per well) were loaded onto a nitrocellulose membrane with a slot-blot apparatus under vacuum pressure. The membrane was blocked for 2 h with a solution of 3% (w/v) bovine serum albumin in PBS containing 0.01% (w/v) sodium azide and 0.2% (v/v) Tween 20 and incubated respectively with primary antibodies anti-3NT (#SAB5200009 Sigma-Aldrich, St. Louis, MO, USA) for 2h at RT. Membranes were washed and incubated with anti-rabbit or mouse IgG alkaline phosphatase secondary antibodies (Sigma-Aldrich, St Louis, MO, USA) for 1 h at room temperature. The membrane was developed with Sigma fast tablets (5-bromo-4-chloro-3-indolyl phosphate/nitroblue tetrazolium substrate [BCIP/NBT substrate], Sigma-Aldrich, St Louis, MO, USA). Membranes were dried and the image was acquired using ChemiDoc XP image system and analyzed using Image Lab software (Bio-Rad Laboratories, Hercules, CA, USA).

Western Blot and Immunoprecipitation.

For immunoprecipitation experiments, 100 □g of protein extracts derived from AD and ND pools were pre-cleared with 10% (w/v) protein A/G (50 □l) (Santa Cruz Biotechnology Inc., Heidelberg, Germany) for 20 min on ice, followed by centrifugation, in order to prevent non-specific binding. Then, 1 µg of antibody against the proteins of interest, CAT (#SC-271803), DRP2 (#SC-30228, Santa Cruz Biotechnology, Dallas, TX, USA) and ANXA2 (#H00000302-M02, Abnova, Taipei city, Taiwan) were added to the samples and incubated overnight at 4°C. Immune complexes were collected by using protein A/G suspension and washed five times with immunoprecipitation buffer. Immunoprecipitated samples were recovered by re-suspending the pellets in Laemmli sample buffer. Proteins were separated by SDS-PAGE followed by immunoblotting on a nitrocellulose membrane (Bio-Rad Laboratories, Hercules, CA, USA). Membranes were blocked for 1 h in 3% bovine serum albumin in TBS-T (0.1m Tris-HCl, pH 7.4, 0.15 M NaCl, and 0.1% Tween 20) and incubated overnight at 4°C with primary antibodies: polyclonal anti-3-NT (#SAB5200009 Sigma-Aldrich, St. Louis, MO, USA). For CAT, IR Dye near-infrared dyes-conjugated secondary antibodies (1:2500; LI-COR, Lincoln,

Nebraska, USA) were used. The immunodetection was performed using a dual-mode Western imaging system Odyssey FC (LI-COR Lincoln, Nebraska, USA). Quantification was performed using Image Studio Software (LI-COR, Lincoln, Nebraska, USA). DRP2, ANXA2 and CAT proteins were detected by the peroxidase-conjugated secondary antibody (1:5000; Sigma–Aldrich, St Louis, MO, USA) with Super Signal West Pico chemiluminescent substrate (Thermo Scientific, Waltham, MA, USA). Membranes were then acquired with Chemi-Doc MP (Bio-Rad) and analyzed using Image Lab software (Bio-Rad). All results were expressed as a ratio between 3-NT and the total amount of the interested proteins (CAT, DRP2 and ANXA2). For western blot analysis, 20 □g of protein extracts derived from AD and ND pools were separated by SDS-PAGE, as mentioned above, and incubated overnight with primary antibodies: CAT (#SC-271803 Santa Cruz Biotechnology, Dallas, TX, USA) and α-tubulin (#T5168 Sigma-Aldrich, St. Louis, MO, USA). IR Dye near-infrared dyes-conjugated secondary antibodies were used and quantification was performed as mentioned above. Results were normalized over the α-tubulin.

Catalase activity

Catalase activity was measured monitoring the decomposition of H_2O_2 according to Shangari and O'Brien [33]. In particular, 20 µg of lymphocyte protein extracts were incubated in a final volume of 100 µl of substrate (65µM hydrogen peroxide in 6.0 mM PBS buffer pH 7.4) at 37°C for 60 s. The enzymatic reaction was stopped by the addition of 100 µl of 32.4 mM ammonium molybdate (Sigma Aldrich, St Louis, MO, USA) and measured at 405nm. The results were extrapolated by a standard curve (ranging from 12U/ml to 0,25 U/ml) performed with purified CAT enzyme (20100 U Sigma Aldrich, St Louis, MO, USA), and expressed as Units/mg of proteins.

Statistical analysis

Statistical analyses of data obtained by PD-QUEST software were performed using Student's t-test. Significance was accepted if the p value < 0.05. All the data are expressed as mean ± SEM of 6-pooled samples. All statistical analyses were performed using GraphPad Prism 5.0 software.

RESULTS

Redox proteomics data

Using a redox proteomic approach, we investigated the 3-NT proteome in human T-lymphocyte population from AD and ND subjects. Before proceeding with the proteomics approach, we analyzed total protein nitration levels in T-cell from AD and ND subjects. Our data demonstrated the increased nitration levels in AD compared to ND T-cells of about 25% (Fig.1). The subsequent redox proteomics analyses led to the identification of 10 proteins statistically more nitrated in AD T-cells compared with their age-matched ND subjects. In Figures 2 and 3 a representative 2D map of nitrated proteins compared with a 2D expression gel are shown. Proteins differently nitrated can be classified according to their functions. The twenty-seven percent of the total nitrated proteins are linked to the cytoskeletal network (Table 2): Annexin A2 (ANXA2; 15.88-fold increase, *p value* 0.011), Annexin A11 (ANXA11; 41.51-fold increase, *p value* 0.0030) and Dihydropyrimidinase-related protein 2 (DRP2, also known as collapsing response mediated protein-2 CRMP2; 5.17-fold increase, *p value* 0.0033). The eighteen percent of the identified nitrated proteins are involved in protein turnover: heat shock cognate 71 (HSC71 or HSPA8; 7.15-fold increase, *p value* 0.043); and two spots were identified as cytosol aminopeptidase (LAP3; respectively with 14.5- and 9.04-fold increase, *p value* <0.05). A further 18% of the proteins are implicated in cellular signaling: Type II inositol 3,4-biphosphate 4-phosphate (INBPP4; 7.82-fold increase, *p value* 0.007); and Phosphatidylinositol-4,5-bisphosphate 3-kinase subunit β (PI3K; 7.40-fold increase, *p value* 0.0013). The remaining proteins are involved, in energy metabolism: ATP synthase subunit α (ATP syn α; 21.52-fold increase, *p value* 0.04); transcriptional regulation: the transcriptional adapter 2-β protein (TADA2B; 18.65-fold increase, *p value* 0.0002); and anti-oxidant response: catalase (CAT; 4.52-fold increase, *p value* 0.02).

DRP2, ANXA2 and CAT increased nitration

Selective nitrated proteins identified by redox proteomics were further analyzed with immunoprecipitation techniques. In particular, DRP2, ANXA2, and CAT were immunoprecipitated with specific antibodies and then immunoblotted with 3-NT antibody.

As shown in Figure 4A, immunoprecipitation analysis of DRP2 demonstrates an increase of 3-NT-DRP2 levels of about 50% more in AD samples compared to ND subjects ($p<0.05$), confirming the redox proteomics results. Similar results were obtained with ANXA2, which showed increased nitration of about 1.5-fold after IP isolation and 3-NT probing (Fig. 4B).

Further, also CAT is more nitrated in AD compared to ND subjects T-cells ($p <0.05$), (Fig. 4C), although the levels of catalase appeared significantly lower in AD than in ND subjects. Thus, total protein extracts derived from AD and ND subjects were further processed for western blot analysis with anti-CAT antibody. As shown in Fig. 5A total catalase (CATtot) was confirmed to be significantly decreased in AD pools compared with ND ones. Interestingly, also its enzymatic activity, measured following the kinetics of H_2O_2 decomposition, was statistically reduced in the AD T lymphocytes than in ND T-cells (AD 0.164 ± 0.082 vs ND 0.241 ± 0.125 $p<0.05$) (Fig. 5C)

STRING analysis

By using STRING software [34, 35], the potential interaction between the proteins identified in our redox proteomics analysis and their combined role in specific molecular pathways and/or molecular functions were analysed. The number of interactions between proteins significantly identified is 13 (PPI enrichment p-value: 0.00959) and was higher than the expected one for a random set of proteins of similar size, meaning that proteins are at least partially biologically connected, as a group (Fig.6). Further, part of the proteins found nitrated in this work might be involved in MHC class II protein complex binding (HSC71 and ANXA11, p= 0.0243) and/or in S100 protein binding (HSC71 and ANXA2, p=0.0243). As far as cellular component pathways, the nitrated proteins identified in this work might be involved in myelin sheath (HSC71, ANXA2, DRP2 and ATP syn α, p= 0.001) and/or in extracellular exosome (LAP3, ATP syn α, CAT, DRP2, HSC71, ANXA2 and ANXA11, p=0.011)

DISCUSSION

Increasing evidence suggests that activation of peripheral immune cells and systemic low-grade inflammation play a role in the brain's pathological events, including

AD [6, 10]. Beyond the molecular alteration related to immune functions, AD lymphocytes were found different from healthy controls in term of increased oxidative stress [36, 37]. For example, protein oxidation markers, such as protein carbonyls and 3-nitrotyrosine, were significantly elevated, and SOD activity was impaired in AD lymphocytes, showing also a negative correlation with MMSE [18]. In addition, the role of NO as an additional signal in the induction of T-cell subset response, suggests that the loop established among inflammatory processes and long-lasting RNS production could be at the basis of the immune-senescence and chronic inflammation involved in the disease development [38-40]. In this context, nitrosative stress might be a potential mechanistic linkage between ageing and AD. Here, we found a significant higher level of the high sensitive CRP (hsCRP) in AD plasma, index of a low-grade inflammation, and a number of highly tyrosine-nitrated proteins in AD T-cells compared to those found in healthy control. These proteins were related to the cytoskeletal network, protein turnover, cellular signaling, energy metabolism and anti-oxidant response. Considering the role that these proteins have in the immune system, and the effects of excessive nitration on protein structure and function, these results could give new insights into AD immune dysfunction and clarify the link between systemic immune alterations and AD pathogenesis. On the other hand, we cannot exclude that redox alterations of blood cells could mimic what occurs in the central nervous system, thus becoming an early warning signal of central oxidative dysfunction [19, 20]. Therefore, we discussed some of these nitrated-proteins considering their function in T lymphocytes and in the context of AD pathogenesis, taking into account whether similar modifications have been found in AD brain previously.

Glucose metabolism/signaling

Our analysis of T-cell nitrated proteome identified the oxidative modification of ATP synthase alpha subunit in AD patients compared to ND subjects (Table 2). Immune functions rely on energy availability with ATP being the principal immediate donor, usually originated via oxidative phosphorylation (OXPHOS) in the mitochondrial respiratory chain and/or aerobic glycolysis [41, 42]. Interestingly, the activation of lymphocytes is associated with a switch to a metabolic phenotype with an increase in both glycolytic function and mitochondrial oxygen consumption [43, 44]. This is essential for

their diverse immunological functions, which includes clonal expansion and the production of cytokines and antibodies [45-47] The fact that ATP synthase alpha subunit was found highly nitrated in AD T-cells corroborates the finding showing that lymphocytes from AD patients exhibit a reduced endogenous basal rate of respiration, as well as a significant impairment of total OXPHOS capacity [48, 49]. Decreased activity of ATP synthase and low levels of electron transport chain complex V also are reported in AD brain [49, 50] . At this regard, studies from Butterfield's laboratory showed that ATP synthase, mainly the alpha-subunit, undergoes 3-NT and HNE modification in MCI and AD brain, likely explaining the reduced activity of ATP synthase and reduced ATP levels [51-54]. Furthermore, in line with other studies [55] we also demonstrated the presence of autoantibodies against ATP synthase in sera and cerebrospinal fluids from AD patients, which could be the result of circulating oxidized ATP synthase [56].

PI3K is involved in T-cell activation throughout a pathway under the control of CD28-dependent signaling, involving Akt (a serine/threonine specific protein kinase), and mechanistic-mammalian target of rapamycin complex 1 (the mTORC1 pathway) [42, 46, 57] Activation of the PI3K/Akt/mTOR pathway is critical to promote the glucose metabolism and aerobic glycolysis essential for cell growth and proliferation and to prevent a state of T-cell hypo-responsiveness known as T-cell energy [57]. Sheu et al. [58], demonstrated that low concentration of several NO donors regulated PI3K activity, while higher amounts negative affected its function. In addition, dysregulation of the PI3K/AKT/mTOR pathway is commonly reported in brains from AD and MCI subjects, meaning this occurs early in the disease progression [59]. The nitration of ATP synthase and PI3K could be, on one side, a mechanism by which increased OS lead to the alteration of energy production in T-cells during AD leading to immunosenescence. On the other side, our data highlight the fact that pathological alterations occurring in AD T- cells reflect changes occurring similarly at brain level, and it supports the hypothesis of Alzheimer as a disease that can be diagnosed systemically.

Cytoskeletal network

Intracellular ANXA2 has been reported to play an important role in exocytosis [60] and endocytosis processes [61, 62]. In addition, this protein is mainly involved in

membrane trafficking [63], lipid raft formation and signal transduction through its interaction with CD44, a cell receptor for hyaluronic acid largely expressed on cell surface of memory T-cells [64]. Previous studies demonstrated that ANXA2 can be nitrated by $ONOO^-$ on tyrosine residues forming tyrosyl radicals, which react to form of dityrosine, altering its functions [65]. Thus, in light of these findings, nitrated-ANXA2 in AD T-cells might contribute to immunosenescence over time. Interestingly, increased expression of ANXA2 protein has been found in AD activated astrocytes, suggesting its role in neuro-inflammation [66]. Whether in the brain ANXA2 is affected by redox -posttranslational modifications, or was dysfunctional, still has not been described.

Little information about ANXA11 is available and notions regarding its structural and functional characteristics are speculated based on similarity with other members of the annexins family. ANXA11 has the highest gene expression in whole blood cells. High expression of ANXA11 in T-cells suggests it may have a significant role in several functions of immune system. Indeed, mutations in ANXA11 have been associated with ALS implicating defective intracellular protein trafficking in disease pathogenesis [67].

DRP2 has essentially been known to specify neuronal polarity and promote axon elongation and branching, by regulating microtubule assembly and reorganizing actin filaments and protein trafficking [68, 69]. It was recently shown that DRP2 is expressed specifically and efficiently in T-cells that need DRP2 to establish a polarized morphology and to engage in subsequent chemokine-directed migration [70, 71]. A correlation between DRP2 expression levels and cell migratory rates toward a chemokine gradient, was in fact demonstrated [70, 71]. DRP2 seems to be involved in favoring T-cell recruitment to inflamed CNS a participating in the T-cell-mediated impairment of neural cell survival and function. Previous proteomic data showed significantly increased protein oxidation levels of DRP2 in Alzheimer's disease brain [53, 72], suggesting that the essential functions of DRP2 in restoring and sustaining plasticity of neuronal connections is compromised in AD brain. A similar outcome is observed in T-cells from AD patients suggesting that, if the role of DRP2 in CNS provides some clues to understand its function in the immune system, its status in T-cells conceivably could predict the development of brain damage during AD onset and progression.

Antioxidant response

Catalase is a heme-containing peroxisome enzyme that breaks down hydrogen peroxide to water and oxygen, with a reaction rate extremely high, capable of decomposing millions of hydrogen peroxide molecules every second [73]. It is a crucial enzyme in protecting the cell against the toxic effects of hydrogen peroxide. On the other hand, its ability to finely and quickly regulate H_2O_2 bursts, implicate this enzyme in many functions in the human body including modulating inflammation [74], differentiation, apoptosis and mutagenesis [75]. Here, we found that CAT was highly nitrated in AD T-cells, but weakly expressed, consistent with the notion that 3-NT bound to CAT contribute to its degradation. This is in line with Keng and colleagues [76], who clearly demonstrated catalase was subjected to degradation following nitration. Therefore, the lower catalase activity found in AD T-cells is in agreement with the higher nitration observed. Similarly, CAT activity was found decreased in AD brain compared with those of healthy subjects, consonant with the hypothesis that similar pathological changes might occur in CNS as well as in peripheral cells [77]. Whether brain catalase activity impairment in AD is due to nitration reaction has not been reported. Mao et al., [78], by using a double-transgenic mouse line MCAT/AβPP (APP Swedish mutation and mitochondria-targeted catalase (MCAT)), demonstrated that overexpression of mitochondrial catalase prevents abnormal APP processing, reduces A□ levels and enhances A□-degrading enzymes in mice. These data provided direct evidence of a key role of CAT-mediated oxidative stress in AD etiopathology.

Protein folding and turnover

HSC71 is recruited by the cell as a primary defense against unfavorable conditions, implicated also in adaptive and innate immunity [79]. HSC71 facilitates the proper folding of newly translated and misfolded proteins and stabilizes or degrades mutant proteins. In AD, the activation of the heat shock response represents a defensive mechanism against amyloid fibril formation. Decreased expression of HSC71 and increased oxidation levels of HSC71 in AD brain were found in several regions of AD brain [52, 80, 81]. Thus, its impairment might be consistent with some of the neuropathological and biochemical abnormalities in this disorder, representing a characteristic feature of AD pathology.

Among the different proteins found to be highly nitrated, some of them are involved in specific pathways that could have a relevance in AD T-cells dysfunction. In particular, by running STRING analysis we observed that the majority of proteins might have a role in extracellular exosome pathway and therefore their increased nitration could lead to the alteration of exosome release from T-cells. It is postulated that extracellular exosomes have important roles in intercellular communication, both locally and systemically, by transferring their contents, including protein, lipids and RNAs, between cells [82]. EEs are involved in numerous physiological processes, and vesicles from both non-immune and immune cells have important roles in immune regulation [83, 84]. Aberrant exosome biogenesis and secretion have been observed in immunological disorders, as well as in neurodegenerative disease, including AD [82]. Within this context, the oxidation of proteins involved in the extracellular exosome pathway in T-cell from AD patients might support a role for altered immune response in the development and progression of AD.

CONCLUSIONS

Overall, our data demonstrate that proteins from T-cells undergo increased nitration during AD as a result of a systemic pro-oxidant environment. Intriguingly, the identification of the specific targets of protein nitration support the potential impairment of crucial pathways involved in cell maintenance and proper function and suggest their potential value as predictors of brain pathological cellular damage.

Acknowledgements

This work was supported by the Ministry of Instruction, Universities and Research (MIUR) under the SIR program n° RBSI144MT to FDD, by Fondi di Ateneo n° RG116154C9214D1A and C26H15JT9X from Sapienza University of Rome to FDD and MP, by funding from the People Programme (Marie Curie Actions) of the European Union's Seventh Framework Programme (FP7/2007-2013) under REA grant agreement n° 624341 to EB and MP; by funding from Banca d'Italia n° 12868/17 to EB; and by Fondazione Cariplo (2014-0769), by University of Brescia (BIOMANE).

ABBREVIATIONS

2D = 2 dimensional

3-NT = 3- nitrotyrosine

AD = Alzheimer Disease

ANX11 = Annexin A11

ANX2 = Annexin A2

ATP Syn α = ATP synthase alpha

CAT = Catalase

DRP2 = Dihydropyrimidinase-related protein 2

HNE = 4- Hydroxynonenal

HSC71 (HSPA8) = Heat shock cognate 71

hsCRP = High sensitivity C-reactive protein

IEF = IsoElectricFocusing

INBPP4 = Type II inositol 3,4-biphosphate 4-phosphate

IP = Immunoprecipitation

LAP3 = Cytosol aminopeptidase

MACS = Magnetic-activated cell sorting

MCI = Mild cognitive impairment

MMSE = Mini-Mental State Examination

MS/MS = Tandem mass spectrometry

ND = Non-demented

OS = oxidative stress

OXPHOS = Oxidative phosphorylation

PI3K = PhosphatidylInositol 3-Kinase

ROS/RNS = Reactive oxygen species / reactive nitrogen species

SOD = Superoxide dismutase

TADA2B = Transcriptional regulation: the transcriptional adapter 2-β protein

WB = Western blot

REFERENCES

[1] A. Serrano-Pozo, M.P. Frosch, E. Masliah, B.T. Hyman, Neuropathological alterations in Alzheimer disease, Cold Spring Harb Perspect Med 1(1) (2011) a006189.
[2] J. Hardy, Alzheimer's disease: The amyloid cascade hypothesis: An update and reappraisal, J Alzheimers Dis 9 (2006) 151-153.
[3] C. Van Cauwenberghe, C. Van Broeckhoven, K. Sleegers, The genetic landscape of Alzheimer disease: clinical implications and perspectives, Genet Med 18(5) (2016) 421-430.
[4] E. Karran, M. Mercken, B. De Strooper, The amyloid cascade hypothesis for Alzheimer's disease: an appraisal for the development of therapeutics, Nat Rev Drug Discov 10(9) (2011) 698-712.
[5] R.J. Hodes, F. Sierra, S.N. Austad, E. Epel, G.N. Neigh, K.M. Erlandson, M.J. Schafer, N.K. LeBrasseur, C. Wiley, J. Campisi, M.E. Sehl, R. Scalia, S. Eguchi, B.S. Kasinath, J.B. Halter, H.J. Cohen, W. Demark-Wahnefried, T.A. Ahles, N. Barzilai, A. Hurria, P.W. Hunt, Disease drivers of aging, Ann N Y Acad Sci 1386(1) (2016) 45-68.
[6] A. Martorana, M. Bulati, S. Buffa, M. Pellicano, C. Caruso, G. Candore, G. Colonna-Romano, Immunosenescence, inflammation and Alzheimer's disease, Longev Healthspan 1 (2012) 8.
[7] I. Baldeiras, I. Santana, M.T. Proenca, M.H. Garrucho, R. Pascoal, A. Rodrigues, D. Duro, C.R. Oliveira, Peripheral oxidative damage in mild cognitive impairment and mild Alzheimer's disease, J Alzheimers Dis 15(1) (2008) 117-28.
[8] F. Di Domenico, R. Coccia, D.A. Butterfield, M. Perluigi, Circulating biomarkers of protein oxidation for Alzheimer disease: expectations within limits, Biochim Biophys Acta 1814(12) (2011) 1785-95.
[9] M. Schrag, C. Mueller, M. Zabel, A. Crofton, W.M. Kirsch, O. Ghribi, R. Squitti, G. Perry, Oxidative stress in blood in Alzheimer's disease and mild cognitive impairment: a meta-analysis, Neurobiol Dis 59 (2013) 100-10.
[10] M. Pellicano, M. Bulati, S. Buffa, M. Barbagallo, A. Di Prima, G. Misiano, P. Picone, M. Di Carlo, D. Nuzzo, G. Candore, S. Vasto, D. Lio, C. Caruso, G. Colonna-Romano, Systemic immune responses in Alzheimer's disease: in vitro mononuclear cell activation and cytokine production, J Alzheimers Dis 21(1) (2010) 181-92.
[11] L. Speciale, E. Calabrese, M. Saresella, C. Tinelli, C. Mariani, L. Sanvito, R. Longhi, P. Ferrante, Lymphocyte subset patterns and cytokine production in Alzheimer's disease patients, Neurobiol Aging 28(8) (2007) 1163-9.
[12] J. Tan, T. Town, L. Abdullah, Y. Wu, A. Placzek, B. Small, J. Kroeger, F. Crawford, D. Richards, M. Mullan, CD45 isoform alteration in CD4+T cells as a potential diagnostic marker of Alzheimer's disease, J Neuroimmunol 132(1-2) (2002) 164-172.
[13] S.R. Xue, D.H. Xu, X.X. Yang, W.L. Dong, Alterations in lymphocyte subset patterns and co-stimulatory molecules in patients with Alzheimer disease, Chin Med J (Engl) 122(12) (2009) 1469-72.
[14] D. Di Bona, A. Plaia, S. Vasto, L. Cavallone, F. Lescai, C. Franceschi, F. Licastro, G. Colonna-Romano, D. Lio, G. Candore, C. Caruso, Association between the interleukin-1 beta polymorphisms and Alzheimer's disease: A systematic review and meta-analysis, Brain Res Rev 59(1) (2008) 155-163.
[15] D. Di Bona, S. Vasto, C. Capurso, L. Christiansen, L. Deiana, C. Franceschi, M. Hurme, E. Mocchegiani, M. Rea, D. Lio, G. Candore, C. Caruso, Effect of interleukin-6

polymorphisms on human longevity: A systematic review and meta-analysis, Ageing Res Rev 8(1) (2009) 36-42.
[16] J. Wojsiat, K.M. Zoltowska, K. Laskowska-Kaszub, U. Wojda, Oxidant/Antioxidant Imbalance in Alzheimer's Disease: Therapeutic and Diagnostic Prospects, Oxid Med Cell Longev 2018 (2018) 6435861.
[17] L. Buizza, G. Cenini, C. Lanni, G. Ferrari-Toninelli, C. Prandelli, S. Govoni, E. Buoso, M. Racchi, M. Barcikowska, M. Styczynska, A. Szybinska, D.A. Butterfield, M. Memo, D. Uberti, Conformational Altered p53 as an Early Marker of Oxidative Stress in Alzheimer's Disease, Plos One 7(1) (2012).
[18] N. Arce-Varas, G. Abate, C. Prandelli, C. Martinez, F. Cuetos, M. Menendez, M. Marziano, D. Cabrera-Garcia, M.T. Fernandez-Sanchez, A. Novelli, M. Memo, D. Uberti, Comparison of Extracellular and Intracellular Blood Compartments High-lights Redox Alterations in Alzheimer's and Mild Cognitive Impairment Patients, Curr Alzheimer Res 14(1) (2017) 112-122.
[19] R. Sultana, M. Baglioni, R. Cecchetti, J. Cai, J.B. Klein, P. Bastiani, C. Ruggiero, P. Mecocci, D.A. Butterfield, Lymphocyte mitochondria: toward identification of peripheral biomarkers in the progression of Alzheimer disease, Free Radic Biol Med 65 (2013) 595-606.
[20] R. Sultana, P. Mecocci, F. Mangialasche, R. Cecchetti, M. Baglioni, D.A. Butterfield, Increased Protein and Lipid Oxidative Damage in Mitochondria Isolated from Lymphocytes from Patients with Alzheimer's Disease: Insights into the Role of Oxidative Stress in Alzheimer's Disease and Initial Investigations into a Potential Biomarker for this Dementing Disorder, J Alzheimers Dis 24(1) (2011) 77-84.
[21] A.V. Gudkov, K.V. Gurova, E.A. Komarova, Inflammation and p53: A Tale of Two Stresses, Genes Cancer 2(4) (2011) 503-16.
[22] F. Di Domenico, G. Cenini, R. Sultana, M. Perluigi, D. Uberti, M. Memo, D.A. Butterfield, Glutathionylation of the pro-apoptotic protein p53 in Alzheimer's disease brain: implications for AD pathogenesis, Neurochem Res 34(4) (2009) 727-33.
[23] A. Cocciolo, F. Di Domenico, R. Coccia, A. Fiorini, J. Cai, W.M. Pierce, P. Mecocci, D.A. Butterfield, M. Perluigi, Decreased expression and increased oxidation of plasma haptoglobin in Alzheimer disease: Insights from redox proteomics, Free Radical Bio Med 53(10) (2012) 1868-1876.
[24] M. Mittal, M.R. Siddiqui, K. Tran, S.P. Reddy, A.B. Malik, Reactive oxygen species in inflammation and tissue injury, Antioxid Redox Signal 20(7) (2014) 1126-67.
[25] S. Bartesaghi, R. Radi, Fundamentals on the biochemistry of peroxynitrite and protein tyrosine nitration, Redox Biol 14 (2018) 618-625.
[26] W. Niedbala, B. Cai, F.Y. Liew, Role of nitric oxide in the regulation of T cell functions, Ann Rheum Dis 65 Suppl 3 (2006) iii37-40.
[27] V.R. Lombardi, L. Fernandez-Novoa, I. Etcheverria, S. Seoane, R. Cacabelos, Association between APOE epsilon4 allele and increased expression of CD95 on T cells from patients with Alzheimer's disease, Methods Find Exp Clin Pharmacol 26(7) (2004) 523-9.
[28] T. Togo, H. Akiyama, E. Iseki, H. Kondo, K. Ikeda, M. Kato, T. Oda, K. Tsuchiya, K. Kosaka, Occurrence of T cells in the brain of Alzheimer's disease and other neurological diseases, J Neuroimmunol 124(1-2) (2002) 83-92.

[29] D.A. Butterfield, T.T. Reed, M. Perluigi, C. De Marco, R. Coccia, J.N. Keller, W.R. Markesbery, R. Sultana, Elevated levels of 3-nitrotyrosine in brain from subjects with amnestic mild cognitive impairment: implications for the role of nitration in the progression of Alzheimer's disease, Brain Res 1148 (2007) 243-8.
[30] F. Mangialasche, M.C. Polidori, R. Monastero, S. Ercolani, C. Camarda, R. Cecchetti, P. Mecocci, Biomarkers of oxidative and nitrosative damage in Alzheimer's disease and mild cognitive impairment, Ageing Res Rev 8(4) (2009) 285-305.
[31] K. Dildar, F. Sinem, E. Gokhan, Y. Orhan, M. Filiz, Serum Nitrosative Stress Levels Are Increased in Alzheimer Disease but Not in Vascular Dementia, Alz Dis Assoc Dis 24(2) (2010) 194-197.
[32] D.A. Butterfield, L.Q. Gu, F. Di Domenico, R.A.S. Robinson, Mass Spectrometry and Redox Proteomics: Applications in Disease, Mass Spectrom Rev 33(4) (2014) 277-301.
[33] N. Shangari, P.J. O'Brien, Catalase activity assays, Curr Protoc Toxicol Chapter 7 (2006) Unit 7 7 1-15.
[34] D. Szklarczyk, J.H. Morris, H. Cook, M. Kuhn, S. Wyder, M. Simonovic, A. Santos, N.T. Doncheva, A. Roth, P. Bork, L.J. Jensen, C. von Mering, The STRING database in 2017: quality-controlled protein-protein association networks, made broadly accessible, Nucleic Acids Res 45(D1) (2017) D362-D368.
[35] L.J. Jensen, M. Kuhn, M. Stark, S. Chaffron, C. Creevey, J. Muller, T. Doerks, P. Julien, A. Roth, M. Simonovic, P. Bork, C. von Mering, STRING 8-a global view on proteins and their functional interactions in 630 organisms, Nucleic Acids Res 37 (2009) D412-D416.
[36] A. Mietelska-Porowska, U. Wojda, T Lymphocytes and Inflammatory Mediators in the Interplay between Brain and Blood in Alzheimer's Disease: Potential Pools of New Biomarkers, J Immunol Res 2017 (2017) 4626540.
[37] U. Wojda, Alzheimer's disease lymphocytes: potential for biomarkers?, Biomark Med 10(1) (2016) 1-4.
[38] A. Martinez-Ruiz, Post-Translational Nitric Oxide-Dependent Modifications In Immune System, Redox Biol 5 (2015) 418-419.
[39] V. Holan, M. Krulova, A. Zajicova, J. Pindjakova, Nitric oxide as a regulatory and effector molecule in the immune system, Mol Immunol 38(12-13) (2002) 989-95.
[40] N. Dugas, J.F. Delfraissy, M. Tardieu, Immune regulatory role of nitric oxide within the central nervous system, Res Immunol 146(9) (1995) 707-10.
[41] Y. Chaban, E.J. Boekema, N.V. Dudkina, Structures of mitochondrial oxidative phosphorylation supercomplexes and mechanisms for their stabilisation, Biochim Biophys Acta 1837(4) (2014) 418-26.
[42] T. Gaber, C. Strehl, B. Sawitzki, P. Hoff, F. Buttgereit, Cellular energy metabolism in T-lymphocytes, Int Rev Immunol 34(1) (2015) 34-49.
[43] P.A. Kramer, S. Ravi, B. Chacko, M.S. Johnson, V.M. Darley-Usmar, A review of the mitochondrial and glycolytic metabolism in human platelets and leukocytes:, Implications for their use as bioenergetic biomarkers, Redox Biology 2 (2014) 206-210.
[44] A.N. Macintyre, J.C. Rathmell, Activated lymphocytes as a metabolic model for carcinogenesis, Cancer Metab 1(1) (2013) 5.
[45] E.L. Pearce, E.J. Pearce, Metabolic pathways in immune cell activation and quiescence, Immunity 38(4) (2013) 633-43.

[46] G.J. van der Windt, E.L. Pearce, Metabolic switching and fuel choice during T-cell differentiation and memory development, Immunol Rev 249(1) (2012) 27-42.
[47] G.J.W. van der Windt, B. Everts, C.H. Chang, J.D. Curtis, T.C. Freitas, E. Amiel, E.J. Pearce, E.L. Pearce, Mitochondrial Respiratory Capacity Is a Critical Regulator of CD8(+) T Cell Memory Development, Immunity 36(1) (2012) 68-78.
[48] J. Wojsiat, K. Laskowska-Kaszub, A. Mietelska-Porowska, U. Wojda, Search for Alzheimer's disease biomarkers in blood cells: hypotheses-driven approach, Biomark Med 11(10) (2017) 917-931.
[49] J. Wojsiat, C. Prandelli, K. Laskowska-Kaszub, A. Martin-Requero, U. Wojda, Oxidative Stress and Aberrant Cell Cycle in Alzheimer's Disease Lymphocytes: Diagnostic Prospects, J Alzheimers Dis 46(2) (2015) 329-50.
[50] H. Kawamata, G. Manfredi, Proteinopathies and OXPHOS dysfunction in neurodegenerative diseases, J Cell Biol 216(12) (2017) 3917-3929.
[51] T. Reed, M. Perluigi, R. Sultana, W.M. Pierce, J.B. Klein, D.M. Turner, R. Coccia, W.R. Markesbery, D.A. Butterfield, Redox proteomic identification of 4-Hydroxy-2-nonenal-modified brain proteins in amnestic mild cognitive impairment: Insight into the role of lipid peroxidation in the progression and pathogenesis of Alzheimer's disease, Neurobiol Dis 30(1) (2008) 107-120.
[52] A. Castegna, V. Thongboonkerd, J.B. Klein, B. Lynn, W.R. Markesbery, D.A. Butterfield, Proteomic identification of nitrated proteins in Alzheimer's disease brain, J Neurochem 85(6) (2003) 1394-1401.
[53] R. Sultana, D. Boyd-Kimball, H.F. Poon, J. Cai, W.M. Pierce, J.B. Klein, M. Merchant, W.R. Markesbery, D.A. Butterfield, Redox proteomics identification of oxidized proteins in Alzheimer's disease hippocampus and cerebellum: An approach to understand pathological and biochemical alterations in AD, Neurobiol Aging 27(11) (2006) 1564-1576.
[54] M. Perluigi, R. Sultana, G. Cenini, F. Di Domenico, M. Memo, W.M. Pierce, R. Coccia, D.A. Butterfield, Redox proteomics identification of 4-hydroxynonenal-modified brain proteins in Alzheimer's disease: Role of lipid peroxidation in Alzheimer's disease pathogenesis, Proteom Clin Appl 3(6) (2009) 682-693.
[55] D. Vacirca, C. Barbati, B. Scazzocchio, R. Masella, G. Rosano, W. Malorni, E. Ortona, Anti-ATP Synthase Autoantibodies from Patients with Alzheimer's Disease Reduce Extracellular HDL Level, J Alzheimers Dis 26(3) (2011) 441-445.
[56] F. Di Domenico, G. Pupo, E. Giraldo, A. Lloret, M.C. Badia, M.E. Schinina, A. Giorgi, D.A. Butterfield, J. Vina, M. Perluigi, Autoantibodies Profile in Matching CSF and Serum from AD and aMCI patients: Potential Pathogenic Role and Link to Oxidative Damage, Curr Alzheimer Res 13(2) (2016) 112-122.
[57] K.A. Frauwirth, J.L. Riley, M.H. Harris, R.V. Parry, J.C. Rathmell, D.R. Plas, R.L. Elstrom, C.H. June, C.B. Thompson, The CD28 signaling pathway regulates glucose metabolism, Immunity 16(6) (2002) 769-77.
[58] M.L. Sheu, K.F. Chao, Y.J. Sung, W.W. Lin, S.Y. Lin-Shiau, S.H. Liu, Activation of phosphoinositide 3-kinase in response to inflammation and nitric oxide leads to the up-regulation of cyclooxygenase-2 expression and subsequent cell proliferation in mesangial cells, Cell Signal 17(8) (2005) 975-84.
[59] A. Tramutola, J.C. Triplett, F. Di Domenico, D.M. Niedowicz, M.P. Murphy, R. Coccia, M. Perluigi, D.A. Butterfield, Alteration of mTOR signaling occurs early in the

progression of Alzheimer disease (AD): analysis of brain from subjects with pre-clinical AD, amnestic mild cognitive impairment and late-stage AD, J Neurochem 133(5) (2015) 739-749.
[60] T. Sarafian, L.A. Pradel, J.P. Henry, D. Aunis, M.F. Bader, The Participation of Annexin-Ii (Calpactin-I) in Calcium-Evoked Exocytosis Requires Protein-Kinase-C, Journal of Cell Biology 114(6) (1991) 1135-1147.
[61] N. Emans, J.P. Gorvel, C. Walter, V. Gerke, R. Kellner, G. Griffiths, J. Gruenberg, Annexin-Ii Is a Major Component of Fusogenic Endosomal Vesicles, Journal of Cell Biology 120(6) (1993) 1357-1369.
[62] E. Morel, J. Gruenberg, The p11/S100A10 Light Chain of Annexin A2 Is Dispensable for Annexin A2 Association to Endosomes and Functions in Endosomal Transport, Plos One 2(10) (2007).
[63] E.B. Babiychuk, A. Draeger, Annexins in cell membrane dynamics. Ca(2+)-regulated association of lipid microdomains, J Cell Biol 150(5) (2000) 1113-24.
[64] S. Oliferenko, K. Paiha, T. Harder, V. Gerke, C. Schwarzler, H. Schwarz, H. Beug, U. Gunthert, L.A. Huber, Analysis of CD44-containing lipid rafts: Recruitment of annexin II and stabilization by the actin cytoskeleton, J Cell Biol 146(4) (1999) 843-54.
[65] W.H. Rowan, 3rd, P. Sun, L. Liu, Nitration of annexin II tetramer, Biochemistry 41(4) (2002) 1409-20.
[66] D.A. Eberhard, M.D. Brown, S.R. VandenBerg, Alterations of annexin expression in pathological neuronal and glial reactions. Immunohistochemical localization of annexins I, II (p36 and p11 subunits), IV, and VI in the human hippocampus, Am J Pathol 145(3) (1994) 640-9.
[67] B.N. Smith, S.D. Topp, C. Fallini, H. Shibata, H.J. Chen, C. Troakes, A. King, N. Ticozzi, K.P. Kenna, A. Soragia-Gkazi, J.W. Miller, A. Sato, D.M. Dias, M. Jeon, C. Vance, C.H. Wong, M. de Majo, W. Kattuah, J.C. Mitchell, E.L. Scotter, N.W. Parkin, P.C. Sapp, M. Nolan, P.J. Nestor, M. Simpson, M. Weale, M. Lek, F. Baas, J.M. Vianney de Jong, A. Ten Asbroek, A.G. Redondo, J. Esteban-Perez, C. Tiloca, F. Verde, S. Duga, N. Leigh, H. Pall, K.E. Morrison, A. Al-Chalabi, P.J. Shaw, J. Kirby, M.R. Turner, K. Talbot, O. Hardiman, J.D. Glass, J. De Belleroche, M. Maki, S.E. Moss, C. Miller, C. Gellera, A. Ratti, S. Al-Sarraj, R.H. Brown, Jr., V. Silani, J.E. Landers, C.E. Shaw, Mutations in the vesicular trafficking protein annexin A11 are associated with amyotrophic lateral sclerosis, Sci Transl Med 9(388) (2017).
[68] H. Zhang, E. Kang, Y. Wang, C. Yang, H. Yu, Q. Wang, Z. Chen, C. Zhang, K.M. Christian, H. Song, G.L. Ming, Z. Xu, Brain-specific Crmp2 deletion leads to neuronal development deficits and behavioural impairments in mice, Nat Commun 7 (2016).
[69] R. Khanna, S.M. Wilson, J.M. Brittain, J. Weimer, R. Sultana, A. Butterfield, K. Hensley, Opening Pandora's jar: a primer on the putative roles of CRMP2 in a panoply of neurodegenerative, sensory and motor neuron, and central disorders, Future Neurol 7(6) (2012) 749-771.
[70] P. Vincent, Y. Collette, R. Marignier, C. Vuaillat, V. Rogemond, N. Davoust, C. Malcus, S. Cavagna, A. Gessain, I. Machuca-Gayet, M.F. Belin, T. Quach, P. Giraudon, A role for the neuronal protein collapsin response mediator protein 2 in T lymphocyte polarization and migration, J Immunol 175(11) (2005) 7650-60.
[71] M. Varrin-Doyer, P. Vincent, S. Cavagna, N. Auvergnon, N. Noraz, V. Rogemond, J. Honnorat, M. Moradi-Ameli, P. Giraudon, Phosphorylation of collapsin response

mediator protein 2 on Tyr-479 regulates CXCL12-induced T lymphocyte migration, J Biol Chem 284(19) (2009) 13265-76.
[72] A. Castegna, M. Aksenov, V. Thongboonkerd, J.B. Klein, W.M. Pierce, R. Booze, W.R. Markesbery, D.A. Butterfield, Proteomic identification of oxidatively modified proteins in Alzheimer's disease brain. Part II: dihydropyrimidinase-related protein 2, alpha-enolase and heat shock cognate 71, J Neurochem 82(6) (2002) 1524-32.
[73] C.D. Putnam, A.S. Arvai, Y. Bourne, J.A. Tainer, Active and inhibited human catalase structures: ligand and NADPH binding and catalytic mechanism, J Mol Biol 296(1) (2000) 295-309.
[74] M. Yabuki, S. Kariya, R. Ishisaka, T. Yasuda, T. Yoshioka, A.A. Horton, K. Utsumi, Resistance to nitric oxide-mediated apoptosis in HL-60 variant cells is associated with increased activities of Cu,Zn-superoxide dismutase and catalase, Free Radic Biol Med 26(3-4) (1999) 325-32.
[75] M. Vuillaume, Reduced oxygen species, mutation, induction and cancer initiation, Mutat Res 186(1) (1987) 43-72.
[76] T. Keng, C.T. Privalle, G.S. Gilkeson, J.B. Weinberg, Peroxynitrite formation and decreased catalase activity in autoimmune MRL-lpr/lpr mice, Mol Med 6(9) (2000) 779-92.
[77] D.L. Marcus, C. Thomas, C. Rodriguez, K. Simberkoff, J.S. Tsai, J.A. Strafaci, M.L. Freedman, Increased peroxidation and reduced antioxidant enzyme activity in Alzheimer's disease, Exp Neurol 150(1) (1998) 40-4.
[78] P. Mao, M. Manczak, M.J. Calkins, Q. Truong, T.P. Reddy, A.P. Reddy, U. Shirendeb, H.H. Lo, P.S. Rabinovitch, P.H. Reddy, Mitochondria-targeted catalase reduces abnormal APP processing, amyloid beta production and BACE1 in a mouse model of Alzheimer's disease: implications for neuroprotection and lifespan extension, Hum Mol Genet 21(13) (2012) 2973-90.
[79] M.F. Tsan, B.C. Gao, Heat Shock Protein and Innate Immunity, Cell Mol Immunol 1(4) (2004) 274-279.
[80] R. Sultana, T. Reed, M. Perluigi, R. Coccia, W.M. Pierce, D.A. Butterfield, Proteomic identification of nitrated brain proteins in amnestic mild cognitive impairment: a regional study, J Cell Mol Med 11(4) (2007) 839-51.
[81] B.C. Yoo, S.H. Kim, N. Cairns, M. Fountoulakis, G. Lubec, Deranged expression of molecular chaperones in brains of patients with Alzheimer's disease, Biochem Biophys Res Commun 280(1) (2001) 249-58.
[82] J. De Toro, L. Herschlik, C. Waldner, C. Mongini, Emerging roles of exosomes in normal and pathological conditions: new insights for diagnosis and therapeutic applications, Front Immunol 6 (2015).
[83] P.D. Robbins, A.E. Morelli, Regulation of immune responses by extracellular vesicles, Nat Rev Immunol 14(3) (2014) 195-208.
[84] M.F.S. Lindenbergh, W. Stoorvogel, Antigen Presentation by Extracellular Vesicles from Professional Antigen-Presenting Cells, Annu Rev Immunol 36 (2018) 435-459.
[85] P.A. Parmelee, P.D. Thuras, I.R. Katz, M.P. Lawton, Validation of the Cumulative Illness Rating Scale in a geriatric residential population, J Am Geriatr Soc 43(2) (1995) 130-7.

Figure Legends:

Figure 1: Total protein 3-NT levels. Bar graph obtained by the analysis of slot blot results. Error bars indicate SEM of six samples per group. Densitometry values shown are given as percentage with respect to ND set as 100% (*$p<0.05$).

Figure 2: Representative 2D gel (left) and blot (right) from ND and AD T-cells samples.

Figure 3: Representative 2D blot from ND and AD T-cells samples. The spots showing significantly increased 3-NT levels in AD samples are labeled. The spot numbers indicated on the maps are the same as those listed in Table 2.

Figure 4: Protein-bound 3-NT levels of DRP-2, ANXA2 and CAT analysed by immunoprecipitation/ Western blot. Loading control is also shown. Error bars reported in the graph indicate SEM of six samples per group. Densitometry values shown are given as percentage with respect to ND set as 100% (*$p<0.05$).

Figure 5: A. Expression levels of CAT between ND and AD T-cells analyzed by WB. Data were normalized on tubulin used as loading control. Error bars reported in the graph indicate SEM for six samples per group. Densitometry values shown are given as percentage with respect to ND set as 100% ($p<0.05$) **B. Analysis of CAT activity in T-cells from ND and AD subjects**. CAT activity is reported as U/mg and error bars indicate SEM of six samples per group (*$p<0.05$).

Figure 6: STRING analysis of proteins identified by redox proteomics. A. Network statistics, including number of nodes, number of edges, average node degree, average local clustering coefficient, expected number of edges and protein-protein interaction (PPI) enrichment p-value, are reported. B. Functional network enrichment considering specific molecular function and/or cellular components. Each of the network identified report pathway description, count in gene set and the false discovery rate. C. and D. interactions

between the proteins identified with aberrant 3-NT levels is shown. Different colors on the protein circles represent the involvement of the proteins in the different networks identified. DPYSL2=DRP2; HSPA8=HSC71; ATP5A1= ATP Syn □□

Fig.1

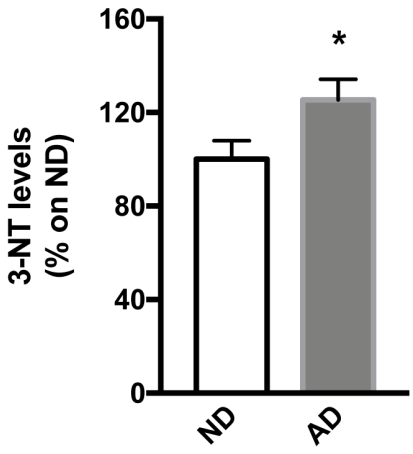
160
120
80
40
0
3-NT levels
(% on ND)
*
ND
AD

Fig.2

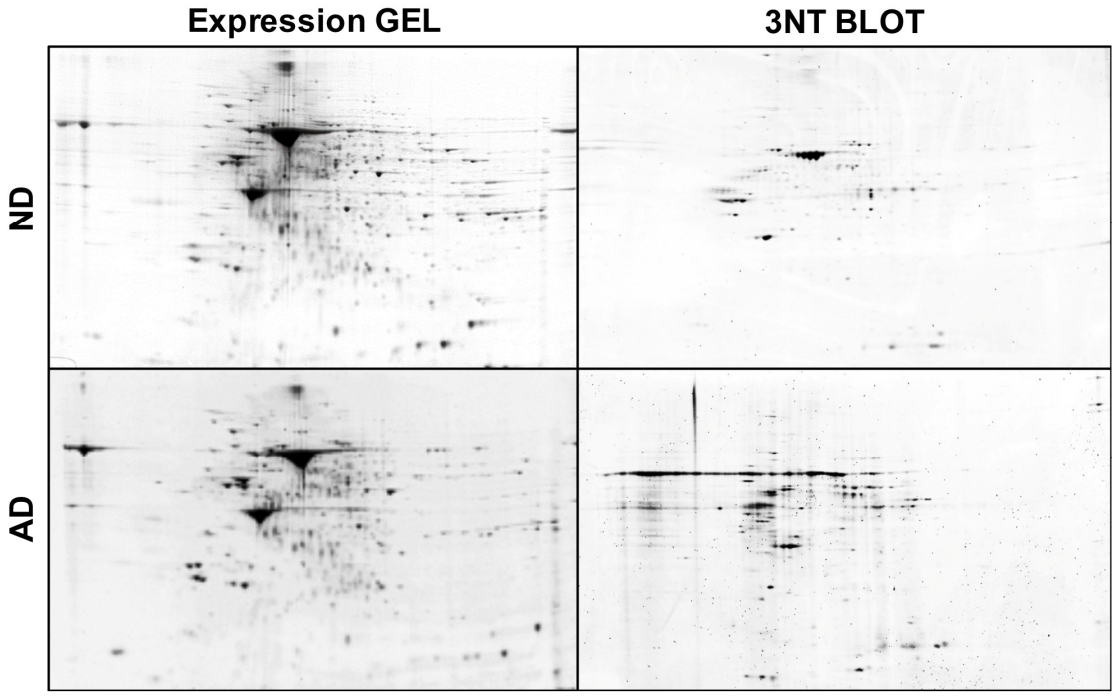
Expression GEL
3NT BLOT
ND
AD

Fig.3

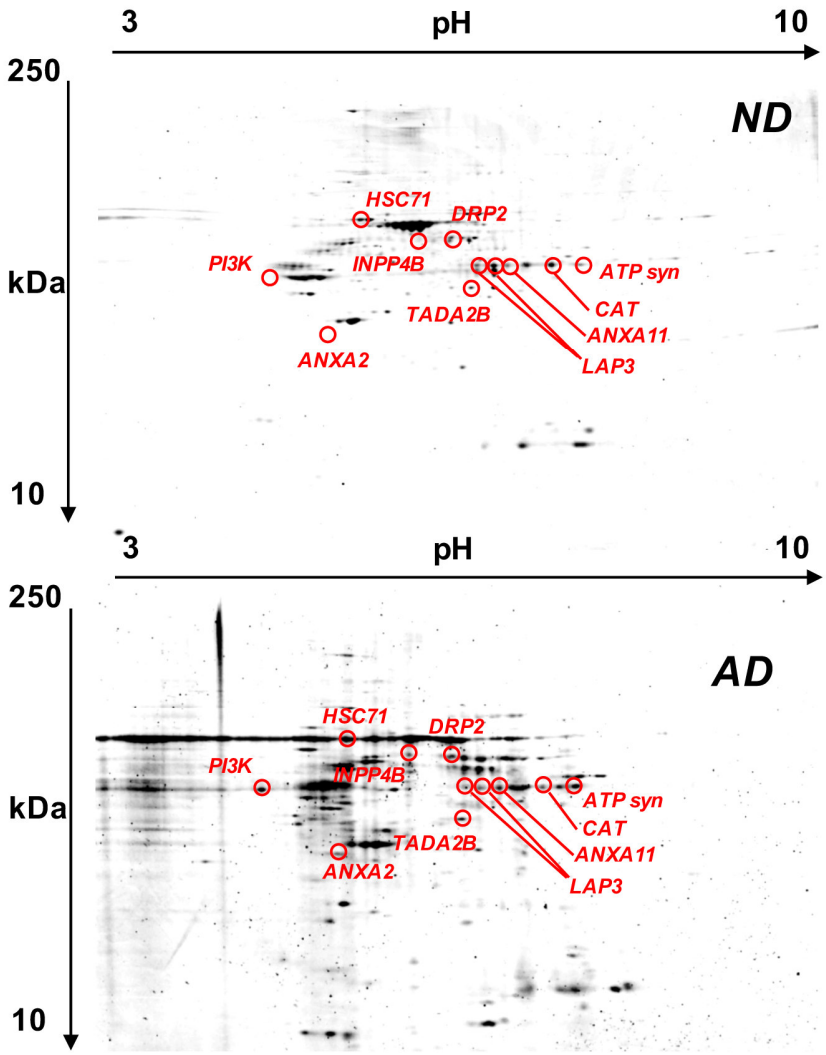
3
pH
10
250
kDa
10
ND
HSC71
DRP2
PI3K
INPP4B
ATP syn
CAT
TADA2B
ANXA11
ANXA2
LAP3
3
pH
10
250
kDa
10
AD
HSC71
DRP2
PI3K
INPP4B
ATP syn
CAT
TADA2B
ANXA11
ANXA2
LAP3

Fig.4

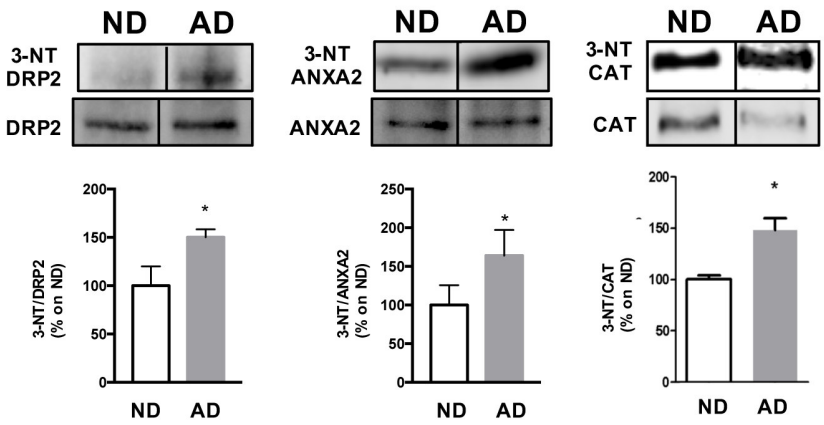
ND
AD
3-NT
DRP2
DRP2
3-NT
ANXA2
ANXA2
3-NT
CAT
CAT
3-NT/DRP2
(% on ND)
3-NT/ANXA2
(% on ND)
3-NT/CAT
(% on ND)
200
150
100
50
0
250
*

Fig.5

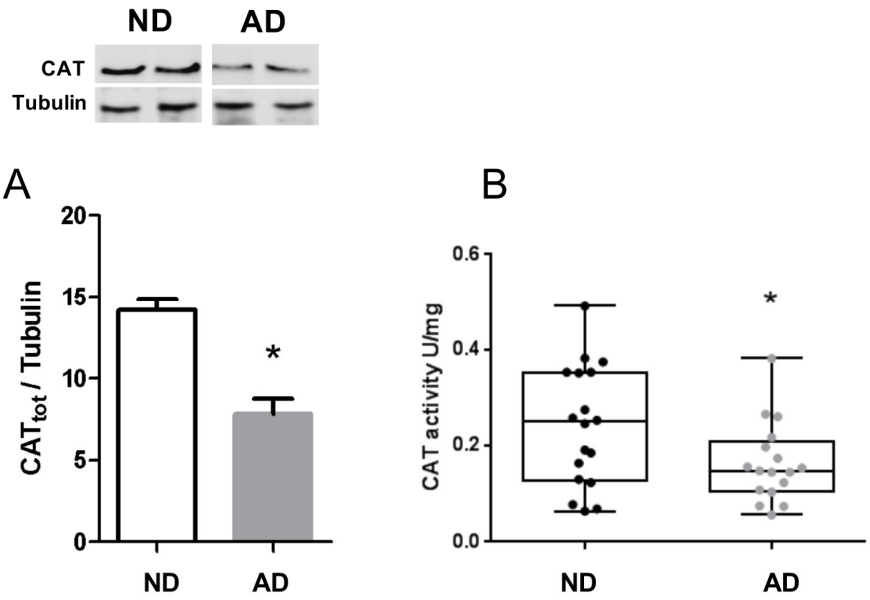
ND
AD
CAT
Tubulin
A
B
CAT$_{tot}$ / Tubulin
CAT activity U/mg
20
15
10
5
0
0.6
0.4
0.2
0.0
*

Fig.6

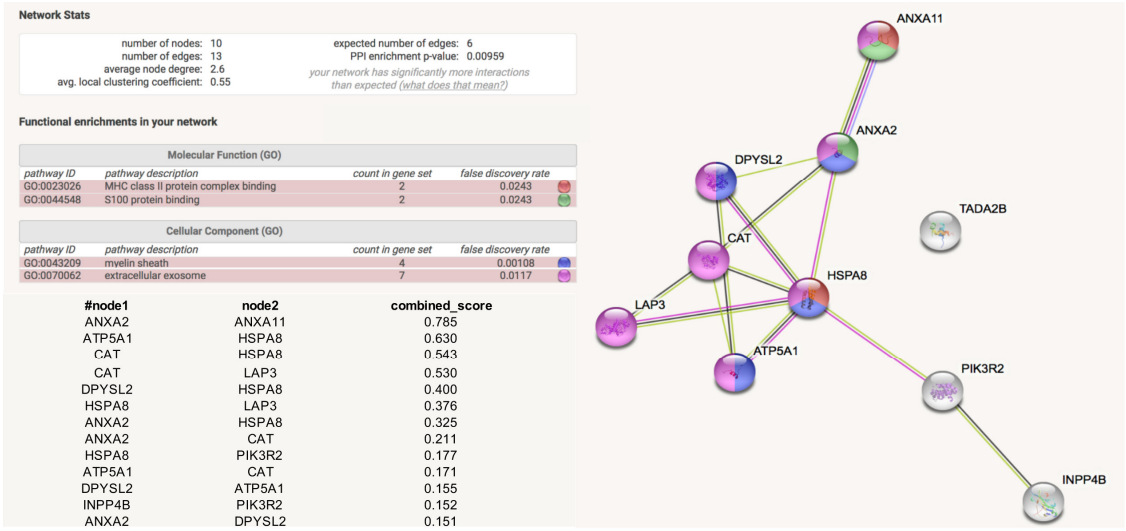

Network Stats

number of nodes: 10
number of edges: 13
average node degree: 2.6
avg. local clustering coefficient: 0.55

expected number of edges: 6
PPI enrichment p-value: 0.00959
your network has significantly more interactions than expected (what does that mean?)

Functional enrichments in your network

Molecular Function (GO)

pathway ID	*pathway description*	*count in gene set*	*false discovery rate*
GO:0023026	MHC class II protein complex binding	2	0.0243
GO:0044548	S100 protein binding	2	0.0243

Cellular Component (GO)

pathway ID	*pathway description*	*count in gene set*	*false discovery rate*
GO:0043209	myelin sheath	4	0.00108
GO:0070062	extracellular exosome	7	0.0117

#node1	node2	combined_score
ANXA2	ANXA11	0.785
ATP5A1	HSPA8	0.630
CAT	HSPA8	0.543
CAT	LAP3	0.530
DPYSL2	HSPA8	0.400
HSPA8	LAP3	0.376
ANXA2	HSPA8	0.325
ANXA2	CAT	0.211
HSPA8	PIK3R2	0.177
ATP5A1	CAT	0.171
DPYSL2	ATP5A1	0.155
INPP4B	PIK3R2	0.152
ANXA2	DPYSL2	0.151

Table 1. Description of demographic and clinical characteristics of enrolled subjects

	ND	**AD**	***p* value**
Subjects *N* (M/F)	19 (11/8)	19 (11/8)	
Mean age (years) ± SD	71.20 ± 6.88	76.94 ± 9.44	0.0095
Mean MMSE (score/ max score= 30) ± SD	30 ± 0	17.56 ± 8.34	< 0.0001
Mean comorbidity index ± SD [85]86]	1.53 ± 0.90	1.73 ± 0.84	0.7924
Inflammatory marker			
hsCRP (mg/L)			
Mean ± SD	0.86 ± 0.64	2.31 ± 2.68	0.0380
Interquartile range	0.33 – 1.39	0.34 – 3.97	

Legend: AD, Alzheimer disease patients; ND, non-demented subjects; N, number of subjects; M, male; F, female; SD, Standard Deviation; MMSE, Mini Mental State Examination; hsCRP, high sensitive C-reactive protein

Table 2: Redox proteomics data

N.	protein	3NT Fold	p value	Uniprot number	score	pI/MW	peptides/ coverage
1	**Phosphatidylinositol 3-kinase regulatory subunit beta** OS=Homo sapiens GN=PIK3R2 PE=1 SV=2 - [P85B_HUMAN]	**7.4**	0.001	O00459	2,33	6,43/81	1/2,61
2	**Annexin A2-like protein** OS=Homo sapiens GN=ANXA2P2 PE=5 SV=2 - [AXA2L_HUMAN]	**2.8**	0.01	P07355	13,75	6,95/38,6	4/12,39
3	**Heat shock cognate 71 kDa protein** OS=Homo sapiens GN=HSPA8 PE=1 SV=1 - [HSP7C_HUMAN]	**7.1**	0.04	P11142	10,24	5,52/70,9	4/7,12
4	**Type II inositol 3,4-bisphosphate 4-phosphatase** OS=Homo sapiens GN=INPP4B PE=2 SV=4 - [INP4B_HUMAN]	**7.8**	0.007	O15327	2,25	6,27/104, 7	2/2,38
5	**Transcriptional adapter 2-beta** OS=Homo sapiens GN=TADA2B PE=1 SV=2 - [TAD2B_HUMAN]	**8.6**	0.0002	Q86TJ2	5,19	7,83/48,4	2/4,52
6 9	**Leucine aminopeptidase** OS=Homo sapiens GN=LAP3 PE=1 SV=3 - [AMPL_HUMAN]	**4.5** **9.0**	0.05 0.018	P28838	2,97 6,74	7,93/56	1/2,97 3/6,74
7	**Dihydropyrimidinase-related protein 2** OS=Homo sapiens GN=DPYSL2 PE=1 SV=1 - [DPYL2_HUMAN]	**2.1**	0.03	Q16555	5,32	6,38/62,3	2/4,20
8	**Annexin A11** OS=Homo sapiens GN=ANXA11 PE=1 SV=1 - [ANX11_HUMAN]	**4.1**	0.003	P50995	2,5	7,65/54,4	1/1,98
10	**Catalase** OS=Homo sapiens GN=CAT PE=1 SV=3 - [CATA_HUMAN]	**4.5**	0.02	P04040	4,97	7,39//59, 7	2/4,36
11	**ATP synthase subunit alpha, mitochondrial** OS=Homo sapiens GN=ATP5A1 PE=1 SV=1 - [ATPA_HUMAN]	**3.5**	0.04	P25705	17,65	9,13/59,7	8/17,65